C. R. Physique 12 (2011) 115–122

Contents lists available at ScienceDirect

Comptes Rendus Physique

www.sciencedirect.com

Propagation and plasmas: new challenges, new applications

Wavenumber spectrum of micro-turbulence in tokamak plasmas

Spectre en nombre d'onde de la micro-turbulence dans les plasmas de tokamak

L. Vermare [a,*], Ö.D. Gürcan [a], P. Hennequin [a], C. Honoré [a], X. Garbet [b], J.C. Giacalone [b], R. Sabot [b], F. Clairet [b], Tore Supra Team [b]

[a] *École polytechnique, LPP, CNRS UMR 7648, 91128 Palaiseau cedex, France*
[b] *CEA, IRFM, 13108 Saint-Paul-lez-Durance, France*

ARTICLE INFO

Article history:
Available online 17 March 2011

Keywords:
Tokamak plasma
Micro-turbulence

Mots-clés :
Plasma de tokamak
Micro-turbulence

ABSTRACT

A better understanding of turbulent transport in a tokamak plasma requires precise comparisons between experimental observation and theoretical prediction of micro-turbulence characteristics. The repartition of fluctuation energy over different spatial scales, which contains detailed information about the character of underlying instabilities and the mechanisms involved in energy transfer between different scales, is one of the few quantities allowing a high detail comparison. The present article reports the investigation performed on the Tore Supra tokamak on the wavenumber spectrum of micro-turbulence using Doppler backscattering. The theoretical approach consists of the derivation of spectral models that include interactions between fluctuations and large scale flow structures.

RÉSUMÉ

Une meilleure compréhension du transport turbulent dans les plasmas de tokamak exige des comparaisons précises entre les observations expérimentales et les prédictions théoriques des caractéristiques de la micro-turbulence. La répartition de l'énergie des fluctuations sur les différentes échelles spatiales, qui contient des informations sur le type instabilités sous-jacentes et sur les mécanismes de transfert d'énergie entre échelles spatiales, est l'une des rares quantités permettant une comparaison de niveau élevé. Cet article présente le travail mené sur le tokamak Tore Supra sur l'étude du spectre en nombre d'onde de la micro-turbulence mesuré par rétro-diffusion Doppler. L'approche théorique consiste en la dérivation de modéles spectraux qui inclut les interactions entre les fluctuations et les structures d'écoulement de grandes échelles.

1. Introduction

The performance of most recent tokamaks are limited by the existence of turbulent transport (also denoted as *anomalous transport*) that results in loss of heat, faster than only through the effect of collisions. The main instabilities that underlie turbulent transport in fusion plasmas are now well identified. The spectrum of such instabilities is quite rich and extend over a large range of spatial scales. At the "large scales" of the micro-turbulence range (i.e. relatively smaller wavenumbers),

* Corresponding author.
E-mail address: laure.vermare@lpp.polytechnique.fr (L. Vermare).

1631-0705/$ – see front matter
doi:10.1016/j.crhy.2010.11.003

the main instabilities are the modes driven by the Ion Temperature Gradient (ITG) and Trapped Electron Modes (TEM), where the latter is driven by the electrons trapped in the low magnetic field side of the machine. Both of these modes develop at spatial scales of the order of the ion Larmor radius (typically $\rho_i = [1\text{ mm}–1\text{ cm}]$). At even smaller scales, there are modes driven by the Electron Temperature Gradient (ETG) with spatial scales around the electron Larmor radius (typically $\rho_e = [10\ \mu\text{m}–100\ \mu\text{m}]$). These micro-instabilities are all driven unstable by density and temperature gradients above a certain threshold.

Nonlinearly, turbulence in the core of tokamak plasmas self-organises through the development of large scale structures that back-react on small scale fluctuations. In particular, two kinds of structures have been identified from numerical simulations of turbulence. In the case of ITG turbulence, the linear instability has a so-called ballooning structure that is extended in the radial direction, commonly named streamers, and leads to rapid rise of the ion heat transport. As back-reaction, large scale sheared flows, called "zonal flows" are nonlinearly generated. These tend to regulate the ion heat transport by shearing apart radially elongated linear structures [1]. The existence of such zonal flows has been confirmed by several observations on different machines (for a complete review see [2]) however their roles in the saturated state still remains to be investigated. In addition, while the experimental level of ion heat transport may roughly be explained by the ITG modes, the role of TEM and ETG in the observed electron heat and particle transport also remain an open question.

A better understanding of turbulent transport requires precise comparisons between experimental observations and theoretical predictions. The repartition of fluctuation energy over different spatial scales, as represented by the wavenumber spectrum, contains detailed information about the character of underlying instabilities and the mechanisms involved in energy transfer between different scales. As a result, wavenumber spectrum is one of the few quantities which allow us a high detail comparison (i.e. a "lower order" in contrast to a comparison, merely of χ_i) between experiment and theory.

The first observations of wavenumber spectra of density fluctuations made in the early eighties, showed that the fluctuation energy is concentrated at ion scales, (i.e. at relatively small wavenumbers, $k\rho_i < 1$) [3–7], which correspond to the range for which ITG/TEM are unstable. At these scales, a difference between the radial direction and the poloidal direction is highlighted [3,5,8]. While the anisotropy is clearly manifest for smaller wavenumbers ($k < 2\ \text{cm}^{-1}$), for the larger wavenumbers, the fluctuation energy follows, in both directions, a power law $S(k) = \delta n^2 \propto k^{-\alpha}$ such as $\alpha \approx -3.5 \pm 1$ [9–13]. This behaviour is generally observed for $k\rho_i \lesssim 1$. Thanks to the extension of the spatial scale range of the measurements, a faster decrease of the energy of fluctuations at higher wavenumbers has been observed, for the first time on the Tore Supra tokamak: the spectrum is composed of two power laws, at small k, $S(k) = k^{-3}$ while from $k\rho_i = [1 - 2]$ $S(k) = k^{-6}$ [14]. Similar spectra have, then, been also observed in W7-AS ($k^{-2.8}$ and $k^{-8.5}$) [15] and in FT-2 ($k^{-2.5}$ and k^{-7}) [16]. This kind of spectrum evokes two-dimensional fluid turbulence in which, in addition to a direct cascade that transfer energy from large to small structures, an inverse cascade takes place. However, the similarity between fluid and magnetized plasma turbulence is rather limited. First, in plasmas, injection appears at various different scales. Secondly, as mentioned above, the development of large-scale structures that interact with the background fluctuations is known to impact the saturated state of turbulence possibly more profoundly than the case of fluid turbulence.

Thanks to the impressive improvement of turbulence simulations through the development of gyro-kinetic description and of computing capabilities, comparisons between experiments and simulations in more and more realistic conditions become possible. In particular, it has been recently shown that wavenumber spectrum obtained from gyrokinetic simulations is consistent with experimental observations [17] for ion turbulence scales ($k\rho_i \lesssim 1$). However, the behaviour of the wavenumber spectrum at smaller scales still remains unresolved.

In this article we present the investigation on the wavenumber spectrum shape that we have performed on the Tore Supra tokamak. In order to increase our understanding of plasma turbulence, we use the experimental and the theoretical approaches, in parallel. The theoretical approach involves the use of simple turbulence model, which allows us to isolate specific mechanisms and to study the impact of these mechanisms separately. Thus, on the one hand, we derive spectral shell models to describe the evolution of turbulence spectrum that include large scale flow structures and the interactions between these structures and fluctuations [18]. On the other hand, we extensively used an efficient and flexible diagnostic, during dedicated experiments, to determine wavenumber spectrum with a combined spatial localization and wavenumber resolution over a large spatial scale range and during a single discharge.

Theoretical background and a description of these spectral shell models are given in Section 2. The experimental approach is then detailed in Section 3. We first present the Doppler back-scattering system installed on Tore Supra and the observation of wavenumber spectrum of density fluctuations and how it compares with theoretical results. Then a discussion on perspective works is proposed in the last section.

2. Theoretical considerations

Theoretical understanding of the form of the wavenumber spectrum in plasma turbulence is nowhere near the understanding of wavenumber spectrum in fluid turbulence. There are different approaches, with different implications about the form of the spectrum, some of which are incompatible with each-other. The quasi-linear approach, which involves balancing the linear growth with a weak-turbulence quasi-linear transfer rate [19,20], gives a spectrum in the linearly driven region and explains roughly the shape of the spectrum near the region of the drive ($k_\perp \rho_s \lesssim 0.5$). However especially near, and just beyond $k_\perp \rho_s \sim 1$, the linear growth linked to ITG/TEM modes (the primary sources of energy injection), is almost completely irrelevant. For instance, for the standard ITG mode, nonlinear transfer dominates over the linear growth

approximately around $k_\perp \rho_s > 0.6$ [17], beyond which the spectrum becomes clearly isotropic. This has various interesting implications. First, if we consider a given scale, the energy that enters that scale does not come directly from the instability (i.e. the for which the background gradient is the free energy source), but rather from the nonlinear transfer. The transfer in plasma turbulence involves a process akin to the standard cascade processes of fluid turbulence. However, in addition disparate scale interactions with large scale structures such as Zonal Flows, Geodesic Acoustic Modes (GAMs) or convective cells, are also likely to play a role in the form of the spectrum.

In order to obtain a simple description, it is common to take plasma turbulence as being two dimensional. This is justified by the fact that the fluctuations are generally rather elongated in the direction parallel to the strong confining magnetic field, and have a locally two-dimensional character for the spatial scales of interest. It is also common to take the electron response as being adiabatic for further simplification when one is concerned with the ion Larmor radius scales. This means that the plasma maintains $\frac{\tilde{n}}{n_0} \approx \frac{e\tilde{\Phi}}{T_e}$, so that the parallel force on electrons is zero. If a fluctuation deviates from this, the electrons move rapidly in the parallel direction and re-establish this state. Note the contradiction here, however. We take the plasma as being 2D (i.e. $\nabla_\parallel \approx 0$), yet we say that in order for the force ($F \approx -T_e \nabla_\parallel (\frac{\tilde{n}}{n_0} - \frac{e\tilde{\Phi}}{T_e})$) to vanish it has to be that $\frac{\tilde{n}}{n_0} \approx \frac{e\tilde{\Phi}}{T_e}$. This is in fact resolved by separating the $k_\parallel = 0$ modes (large scale structures, denoted here by $\bar{\Phi}$), from those that have small but nonzero $k_\parallel$ (denoted actually by $\tilde{\Phi}$), that is $\Phi = \bar{\Phi} + \tilde{\Phi}$, and compute the force only from this fluctuating component whose $k_\parallel$ is small but nonvanishing.

2.1. Potential vorticity conservation

The simplest two-dimensional theoretical models of plasma turbulence are reduced fluid models, such as Hasegawa–Mima [21], or Hasegawa–Wakatani [22] models, which are akin to some of the simplest geophysical fluid dynamics (GFD) models such as the Charney model (see for instance [23] for the detailed analogy). The mathematical similarity between these two physically very different systems can be emphasized in particular by using potential vorticity (PV) description. It can be shown that, nonlinear dynamics in these reduced systems conserve potential vorticity.

In the case of fusion plasmas, the potential vorticity defined as $h \equiv n_i^{gc} \approx n - \rho_s^2 \nabla^2 (\frac{e\Phi}{T_e})$ (and is linked to the ion guiding center density n_i^{gc}) is indeed conserved:

$$\frac{\mathrm{d}h}{\mathrm{d}t} = 0$$

In principle, after solving for h, the adiabatic electron response $\frac{\tilde{n}}{n_0} \approx \frac{e\tilde{\Phi}}{T_e}$ can be used to revert the solution that is found for PV in terms of density:

$$\tilde{h}_k = \left(1 + k^2\right)\tilde{\Phi}_k$$

in normalized units (i.e. $x \to x'/\rho_s$, $t = t'\Omega_i$, $\Phi \to e\Phi'/T_e$, $n \to n'/n_0$ etc. where the primed coordinates have physical units). We shall use the conservation of potential vorticity in order to formulate our simple shell model that permits a computation of the wavenumber spectrum when the interaction with the large scale flows are dominant.

2.2. Shell model and wavenumber spectrum

Once it is established that PV conservation is a good approximation to turbulent plasma dynamics, one can use it to build a simple shell model. Such models, which are based on homogeneous, isotropic turbulence, and local interactions are used commonly in fluid dynamics and they can be used to

1. obtain the steady state spectrum by finding the fixed points of the shell model
2. study nonlinear dynamics, intermittency etc. by numerically integrating them in time

In order to be applicable to fusion plasma systems we include local as well as disparate scale interactions. Since we are interested mainly on the small scales, we integrate over the large scale structures as a single $k_\parallel = 0$ mode with an average perpendicular wavenumber denoted by q.

Nonlinear interactions in a PV conserving system, or the particular example of Hasegawa–Mima model, conserve energy and generalized enstrophy. Similarly the nonlinear interactions in Hasegawa–Wakatani model conserve kinetic and internal energies and a generalized helicity-like term involving both density and electrostatic potential. When the disparate scale interactions with a large scale flow are allowed, the main conserved quantity takes the form of potential enstrophy (i.e. $W = h^2$). Note that it is the "total" potential enstrophy (fluctuations + large scale flows) that is conserved, which suggests that it is in fact potential enstrophy that is exchanged between fluctuations and large scale flows.

Taking $k_n = g^n k_0$ where $g > 1$ is a parameter denoting shell spacing, above observations allow us to build a shell model that conserves potential enstrophy. The model has the form [18,24]:

$$\frac{\partial}{\partial t} h_n - \gamma_n h_n - \alpha p k_n \left(\bar{\Phi} h_{n+1} - g^{-1} \bar{\Phi} h_{n-1}\right) = \alpha p k_n \left(\bar{h} \Phi_{n+1} - g^{-1} \bar{h} \Phi_{n-1}\right) + C(h, \Phi) \tag{1}$$

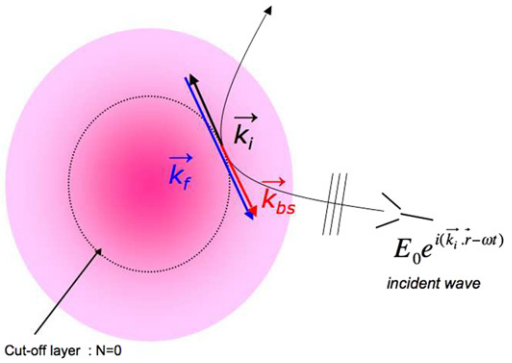

Fig. 1. Illustration of the principle of the Doppler backscattering system.

where γ_n represent linear growth and α is a "free" parameter for the shell-model, representing the strength of the nonlinear term. Here the wave collision term:

$$C(h,\Phi) \equiv \alpha' k_n^2 \left\{ g^{-3}(\Phi_{n-2}h_{n-1} - \Phi_{n-1}h_{n-2}) - g^{-1}(\Phi_{n-1}h_{n+1} - \Phi_{n+1}h_{n-1}) + g(\Phi_{n+1}h_{n+2} - \Phi_{n+2}h_{n+1}) \right\} \tag{2}$$

describes the local cascade. The mean PV equation can be written as:

$$\frac{\partial}{\partial t}\bar{h} - \sum_n \alpha g^{-1} k_n (\Phi_n h_{n-1} - \Phi_{n-1} h_n) = 0 \tag{3}$$

The model as given by (1)–(3), describes the coupled evolution of large and small scales. Of course one should also add a damping term (or take γ_n as being negative) for large n (i.e. large k). If we use $h_n \sim \Phi_n(1+k_n^2)$ one can show that $\Phi_n \sim k_n^{-4/3}$ and $\Phi_n \sim k_n^{-2}$ make $C(h,\Phi)$ vanish exactly. This means that the solution when the local interactions dominate has the basic form $E(k) \propto \{k^{-5}, k^{-11/3}\}(1+k^2)$. In contrast, when the disparate scale interactions with $\bar{\Phi}$ are dominant we find that $h_n \propto k^{-1/2}$, which gives $W(k) \propto k^{-2}$. If we interpret potential enstrophy as enstrophy and link it to the Euler 2D problem, this is apparently equivalent to the Saffman's solution [25] written for enstrophy. Now if we relate $W(k)$ to the discrete Fourier transform, and note that $W(k) \sim |h_{\mathbf{k}}^2|k$, where $h_{\mathbf{k}} \propto (1+k^2)\Phi_{\mathbf{k}}$ and that $\Phi_{\mathbf{k}} \approx n_{\mathbf{k}}$ we find that

$$|n_{\mathbf{k}}|^2 \propto |\Phi_{\mathbf{k}}|^2 \propto \frac{k^{-3}}{(1+k^2)^2} \tag{4}$$

This is the spectrum, when the disparate scale interactions dominate over the local interactions in plasma turbulence. We obtained it here as the solution of a simple shell model in the limit when the local interactions are dropped. In fact, the result is more generic, and is simply due to the form of the nonlinearity as modified by the fact that the electrons cannot respond to large scale modes and the nonlinear interactions are mediated by the large scale flows.

3. Doppler back-scattering system

Different types of diagnostic systems are generally used in order to measure and characterize density fluctuations in hot magnetized plasmas where probes and cameras are not usable. Among those are two major diagnostic families which rely on scattering of electromagnetic waves on plasma fluctuations. On one hand, there is reflectometry that uses microwave frequency range to obtain a cut-off layer inside the plasma. In this case, the probing wave reflected from the plasma is detected and analysed to extract information about the density fluctuations in the vicinity of the cut-off layer (the layer where the refractive index vanishes and the probing wave gets reflected). Major advantages of this method are high sensitivity and excellent localization of the measurement. On the other hand, there are wave-scattering systems based on the detection of probing waves scattered by the fluctuations of the plasma [3,26,27]. The choice of the angle between the emitter and the receptor, permits selecting the spatial scale of the detected fluctuations (elastic scattering). This selectivity in wavenumber is the main advantage of this kind of system.

The Doppler backscattering system combines advantages from both reflectometry and scattering techniques. It is based on the detection of the field backscattered on density fluctuations in the vicinity of the cut-off layer. In practice, the probing wave is chosen in the microwave range and is launched in oblique incidence with respect to the normal of iso-index surfaces (angle α) thereby only the back-scattered signal (no or little reflected signal is received) is detected by the emitter antenna, which also serves as a receptor. The fluctuations whose wavenumber matches the Bragg rule $\vec{k}_f = -2\vec{k}_i$ are selected exclusively, where $\vec{k}_i$ and $\vec{k}_f$ are the local wave-vectors of the probing beam and the density fluctuations respectively (cf. Fig. 1). This technique thus provides the instantaneous spatial Fourier analysis of density fluctuations, $\tilde{n}(\vec{k},t) = \int_V n(\vec{r},t)e^{i\vec{k}.\vec{r}}d\vec{r}$, acting as a band pass filter in k-space around $k = k_0 \sin\alpha$ at the cut-off layer. The radial localization of the measurements

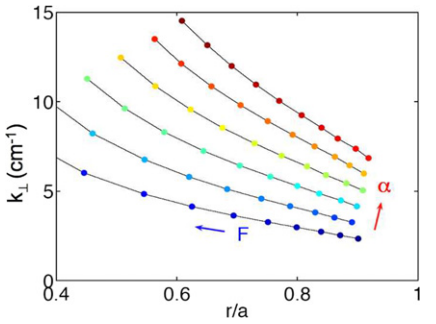

Fig. 2. Mapping r/a vs. k of Doppler backscattering system (V-band, O-mode) measurements for a typical Tore Supra discharge.

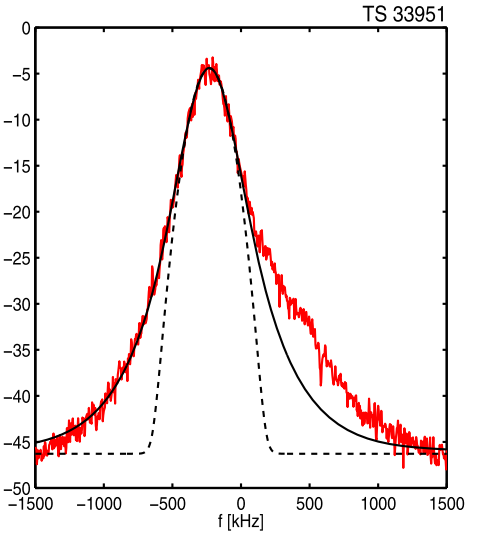

Fig. 3. Frequency spectrum of density fluctuations measured using Doppler backscattering system. The spectrum is Doppler shifted with $V_\perp = 2\pi f_D$.

is provided by two combined effects: a propagation effect and an effect linked to an intrinsic characteristic of the plasma turbulence. First, back-scattering processes are strongly amplified close to the cut-off layer due to swelling of the incident field near the cut-off layer. Secondly, the physical fluctuation energy in the large radial wavenumbers (that interact with the incident beam along the beam trajectory towards the cut-off layer) is quite low, leading to a good localization of the measurement.

The system installed on Tore Supra has two channels [28]: one channel operates in V-band range of frequencies in ordinary polarisation while the second one covers the W-band in extra-ordinary polarisation. These channels allow us, respectively, to probe the plasma from $r/a = 0.5$ to $r/a = 0.9$ (where $r/a = 0$ is the center of the plasma and $r/a = 1$ corresponds to the last closed flux surface) for wavenumber $k = 3$–20 cm^{-1} and from $r/a = 0.85$ to $r/a = 1$ with $k =$ 2–25 cm^{-1}. Gaussian optics are used to control the scattering volume (for more details see [29]). However, due to the long distance between the antenna and the plasma, the waist of the Gaussian beam remains distant from the scattering zone in contrast with the conditions of the analysis of optical mixing in scattering experiments reported in [30] and with other similar systems [31,32].

The radial position and the wavenumber of the probing wave at the cut-off layer are determined using a 3D beam tracing code [33] simulating the propagation of a Gaussian beam in a stationary plasma represented by a radial density profile (measured using fast-sweep reflectometers [34]) and an equilibrium profile of the magnetic field (only needed in the case of extra-ordinary polarisation). An example of measurements mapping for a typical Tore Supra discharge is shown on Fig. 2. The wavenumber selectivity $\triangle k$ is related to the refraction of the Gaussian beam during its propagation and can be evaluated directly from the beam tracing code [35,36].

The power spectral density is Doppler shifted $\triangle\omega = \vec{k}_f.\vec{v}_f$ due to the perpendicular (to the field lines) movement of density fluctuations (cf. Fig. 3). This property allows us to determine the fluctuation velocity at the cut-off layer and is the most currently used property by present Doppler systems for studying plasma flows [37], radial electric field profile [38,39] and instantaneous velocity field [31,40].

The integration of the power spectral density gives the power of fluctuations contained at a radial position and at a specific spatial scale. The measurement of spectra at a large number of couple $(F, \alpha) \leftrightarrow (r, k)$ allow us to resolve the

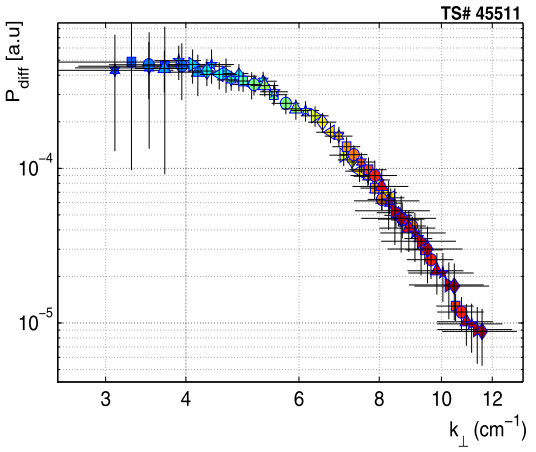

Fig. 4. Example of wavenumber spectrum measured on Tore Supra discharge.

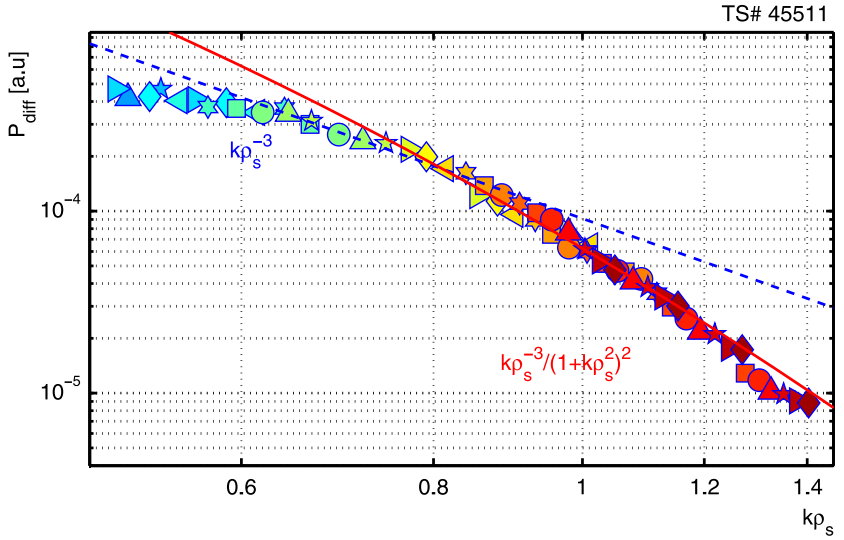

Fig. 5. Experimental wavenumber spectrum of density fluctuations during the discharge 45 511 compared with power law $k\rho_s^{-3}$ (in blue) and the shell model $k\rho_s^{-3}/(1+k\rho_s^2)^2$ (in red).

wavenumber spectrum with a very high discretization such as the one plotted in Fig. 4. Error-bars reported on this figure are evaluated as follows. As mentioned just above the selectivity in k is evaluated directly from the beam tracing code. Then uncertainties on the radial density profile must be also taken into account to determine the resolution in k. The evaluation of the uncertainties on the δn^2 is less trivial. First, there is an impact of the amplitude of the incident signal that differs for each probing frequency. This is corrected using a calibration technique which is not completely perfect and that must be included in the evaluation of the error bars. Secondly, the efficiency of back-scattering processes may be wavenumber dependent. This effect seems to be relevant, only for very small wavenumbers [41–43]. Finally, a small uncertainty coming from the integration process must be included as well.

4. Shape of the wavenumber spectrum

Thanks to the steady-state operation of the Tore Supra tokamak and to the flexibility of the Doppler backscattering system installed on it, we can scan a large number of probing frequency and incident angle pairs (F, α) and obtain the wavenumber spectrum with a high level of resolution in terms of wavenumber discretization. Fig. 5 presents the wavenumber spectrum of density fluctuations measured around $r/a = 0.8 \pm 0.08$ during the discharge #45 511. This spectrum corresponds to a typical discharge of Tore Supra at $B = 3.8$ T, in which the plasma is heated using Ion Cyclotron Resonance Heating system and performed during dedicated experiments (to study the impact of dimensionless parameters such as $\nu*$ on transport and turbulence). As shown in Fig. 5, at small wavenumber ($k\rho_s \leqslant 0.6$) the spectrum seems to saturate. This behaviour corresponds to the characteristic feature of the linear part of the spectrum as discussed in Section 2 and is roughly consistent with a Gaussian shape, thought to be linked to the linear growth rate of the ITG/TEM mode. In

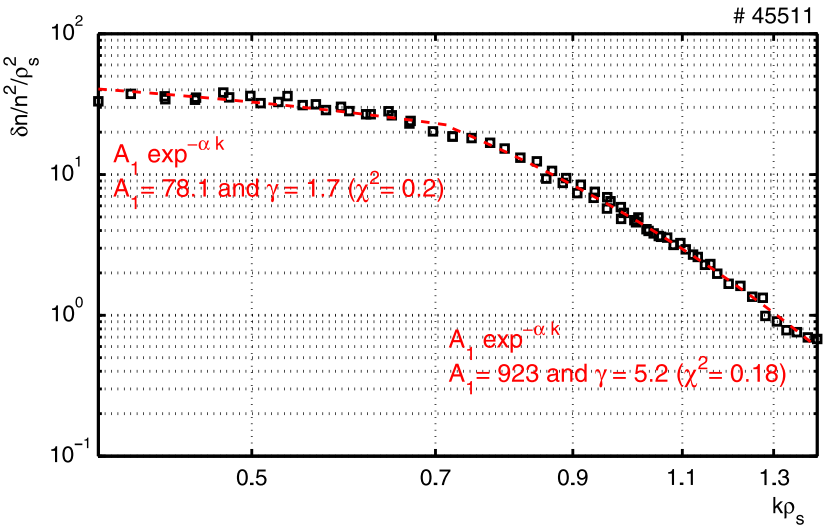

Fig. 6. Experimental wavenumber spectrum of density fluctuations of the discharge 45 511 (in black squares) fitted using two exponential functions.

contrast, for the range of wavenumbers $k\rho_s = [0.6–0.9]$, it follows a power law as $s(k) \propto k^{-3}$ and starts to decrease faster for higher wavenumbers, consistently with previous observations [14]. This form is correctly described using the shell model (4) for $k\rho_s = [0.7–1.2]$. Note that the shell model expression does not have any fitting parameters (apart from the fluctuation level). Therefore, the correct agreement between experiment and this model is remarkable and suggests that interaction between disparate scales including zonal flows is an important ingredient to determine the wavenumber spectrum shape. As already noticed in [14], the wavenumber spectrum may also be fitted using exponential functions. Fig. 6 presents the same wavenumber spectrum as before, but this time fitted using two separate exponential functions. For the smaller wavenumber ($k\rho_s < 0.7$), the measurements are well fitted using an exponential as $e^{-1.7k\rho_s}$. This wavenumber range corresponds to the anisotropic part of the spectrum and is labelled in the figure as the "linear part". Although nonlinear processes inevitably affect this region as well, it appears mainly as the region of energy injection from the plasma micro-instability, driven unstable by gradients in background profiles. In the range of larger wavenumbers, where the nonlinear interactions and the energy transfer dominate, the spectrum has the form: $e^{-5.2k\rho_s}$. This region is akin to the inertial range in fluid turbulence, even though the dominant mechanism for energy transfer may be different and some residual instabilities may exist in this region, due to the final form of the spectrum, the energy these instabilities can inject (i.e. $\propto \gamma_k P$) is quite small.

5. Results and discussion

The wavenumber spectrum gives the repartition of fluctuation energy over different spatial scales. In the present study, we use the wavenumber spectrum of density fluctuations to obtain detailed information about the character of underlying instabilities and to study the mechanisms involved in energy transfer between different scales. For this end, we employed an experimental approach using the Doppler backscattering system installed on the Tore Supra tokamak, which allow us to diagnose the shape of the wavenumber spectrum, accurately, over various discharges. In addition, we employed a theoretical approach based on the study of nonlinear transfer using simple shell models, derived from reduced descriptions of plasma turbulence based on conservation of potential vorticity. During the experimental studies, where various plasma conditions are tested, two main characteristics of the spectrum has been noted. We observed first that the wavenumber spectrum is composed of two regions: at the smaller wavenumbers ($k\rho_s < 0.7$), a region of energy injection from the main instability/instabilities where the spectrum is rather flat and decreases slowly in our range of observation; at larger wavenumbers ($k\rho_s > 0.7$), a region of energy transfer in which the spectrum decreases in a steady fashion. Secondly, the shape of the spectrum in this energy transfer range is found to be well described by the simple form $k^{-3}/(1+k^2)^2$ (Eq. (4)) suggesting that the interactions between large scale flow structures and fluctuations may play an important role in determining the wavenumber spectrum shape. However, note that this part of the spectrum is also well represented by an exponential function. These results lead to a picture of wavenumber spectrum different from that of fluid turbulence. While in the standard picture of fluid turbulence, the energy transfer takes place mainly via local cascade processes, in magnetized plasmas, nonlocal interactions between disparate scales seem to play a dominant role in determining the form of the spectrum. In particular the interactions between small scale fluctuations and large scale flow structures that are driven by the turbulence/instabilities themselves appear to be rather important. In addition, in plasma turbulence, the injection of energy is intrinsic, driven by micro-instabilities and may be important at various different scales while in the standard fluid dynamical study of turbulence the energy injection is usually taken to be well localized in k-space and is assumed to be externally sustained. Another difference between turbulence spectrum in fluids and plasmas comes from the dissipation processes: in fluid turbulence, dissipation of the forward cascading conserved quantity (such as energy for 3D turbulence or enstrophy

for 2D turbulence) affects only small scales while in plasmas, kinetic effects such as Landau damping may appear at various scales depending on the details of parallel dynamics. Finally, the conserved quantities are different. In 2D fluid description, the enstrophy is the main invariant that cascades forward, whereas in plasma turbulence, formulated as a reduced 2D turbulence problem, it is the potential enstrophy that is conserved. In order to characterize the energy injection range and the effects of changing the energy injection on the energy transfer range (or more accurately, potential enstrophy transfer range) one should investigate the effects of changing various plasma parameters. Studying the impact of relevant plasma parameters (such as collisionality, normalized Larmor radius etc.) on the wavenumber spectrum shape, will allow future research to identify the importance of linear phenomena (which is sensitive to plasma parameters) vs. nonlinear processes (which is insensitive to plasma parameters). Moreover, the question of electron thermal transport, and therefore the detection of small scale turbulence, linked possibly to ETG modes at a detail and resolution comparable to that of ion turbulence remains as an important and interesting challenge.

Acknowledgements

This work was carried out within the framework the European Fusion Development Agreement (EFDA) and the French Research Federation for Fusion Studies (FR-FCM). It is supported by the European Communities under the contract of Association between Euratom and CEA. The views and opinions expressed herein do not necessarily reflect those of the European Commission. Financial support was also received from Agence Nationale de la Recherche under contract ANR-06-BLAN-0084.

References

[1] Z. Lin, T.S. Hahm, W.W. Lee, W.M. Tang, R.B. White, Science 281 (1998) 1835.
[2] G.R. Tynan, A. Fujisawa, G. McKee, Plasma Physics and Controlled Fusion 51 (2009) 113001.
[3] C. Surko, R. Slusher, Phys. Rev. Lett. 37 (1976) 1747.
[4] R. Watterson, R. Slusher, C. Surko, Phys. Fluids 28 (1985).
[5] C. Ritz, D. Brower, T. Rhodes, R. Bengtson, S. Levinson, J.N.C. Luhmann, W. Peebles, E. Powers, Nuclear Fusion 27 (1987).
[6] D. Brower, W. Peebles, J.N.C. Luhmann, Nuclear Fusion 27 (1987).
[7] H. Weisen, C. Hollenstein, R. Behn, Plasma Physics and Controlled Fusion 30 (1988) 293.
[8] R.J. Fonck, G. Cosby, R.D. Durst, et al., Phys. Rev. Lett. 70 (1993) 3736.
[9] A. Semet, A. Mase, W.A. Peebles, N.C. Luhmann, S. Zweben, Phys. Rev. Lett. 45 (1980) 445.
[10] TFR-Group, A. Truc, Plasma Physics and Controlled Fusion 26 (1984) 1045.
[11] P. de Simone, D. Frigione, F. Orsitto, Plasma Physics and Controlled Fusion 28 (1986) 751.
[12] F. Gervais, in: 19th EPS Conf. Plasma Phys., 1992.
[13] S. Paul, N. Bretz, R. Durst, R. Fonck, Y. Kim, E. Mazzucato, R. Nazikian, Phys. Fluids B 4 (1992).
[14] P. Hennequin, R. Sabot, C. Honoré, et al., Plasma Physics and Controlled Fusion 46 (2004) B121.
[15] N. Basse, IEEE Trans. Plasma Sci. 36 (2008) 458.
[16] A.D. Gurchenko, E.Z. Gusakov, D.V. Kouprienko, S. Leerink, A.B. Altukhov, J.A. Heikkinen, S.I. Lashkul, L.A. Esipov, A.Y. Stepanov, Plasma Physics and Controlled Fusion 52 (2010) 035010.
[17] A. Casati, T. Gerbaud, P. Hennequin, C. Bourdelle, J. Candy, F. Clairet, X. Garbet, V. Grandgirard, O.D. Gürcan, S. Heuraux, et al., Phys. Rev. Lett. 102 (2009) 165005.
[18] Ö.D. Gürcan, P. Hennequin, L. Vermare, X. Garbet, P.H. Diamond, Plasma Physics and Controlled Fusion 52 (2009) 045002.
[19] T.S. Hahm, W.M. Tang, Phys. Fluids B 3 (1991) 989.
[20] N. Mattor, P.H. Diamond, Phys. Fluids B 1 (1989) 1980.
[21] A. Hasegawa, K. Mima, Phys. Fluids 21 (1978) 87.
[22] A. Hasegawa, M. Wakatani, Phys. Rev. Lett. 50 (1983) 682.
[23] W. Horton, A. Hasegawa, Chaos: An Interdisciplinary Journal of Nonlinear Science 4 (1994) 227.
[24] Ö.D. Gürcan, X. Garbet, P. Hennequin, P.H. Diamond, A. Casati, G.L. Falchetto, Phys. Rev. Lett. 102 (2009) 255002.
[25] P.G. Saffman, Studies in Applied Mathematics 50 (1971) 377.
[26] E. Mazzucato, Phys. Rev. Lett. 36 (1976) 792.
[27] A. Truc, A. Quemeneur, P. Hennequin, et al., Rev. Sci. Inst. 63 (1992) 3716.
[28] P. Hennequin, C. Honoré, A. Truc, et al., Rev. Sci. Inst. 75 (2004) 3881.
[29] P. Hennequin, C. Honoré, A. Truc, A. Quéméneur, C. Fenzi-Bonizec, C. Bourdelle, X. Garbet, G. Hoang, the Tore Supra Team, Nuclear Fusion 46 (2006) S771.
[30] E. Holzhauer, J. Massig, Plasma Physics 20 (1978) 867.
[31] M. Hirsch, E. Holzhauer, Plasma Physics and Controlled Fusion 46 (2004) 593.
[32] V. Bulanin, M. Efanov, Plasma Physics Reports 32 (2006) 47.
[33] C. Honoré, P. Hennequin, A. Truc, A. Quemeneur, Nuclear Fusion 46 (2006) S809.
[34] F. Clairet, C. Bottereau, J. Chareau, R. Sabot, Rev. Sci. Inst. 74 (2003) 1481.
[35] M. Hirsch, E. Holzhauer, J. Baldzuhn, B. Kurzan, Rev. Sci. Inst. 72 (2001) 324.
[36] V. Bulanin, in: 29th EPS Conf. Plasma Phys., vol. 26B, 2002.
[37] P. Hennequin, in: 26th EPS Conf. Plasma Phys., 1999.
[38] G.D. Conway, J. Schirmer, S. Klenge, W. Suttrop, E. Holzhauer, the ASDEX Upgrade Team, Plasma Physics and Controlled Fusion 46 (2004) 951.
[39] E. Trier, L.G. Eriksson, P. Hennequin, C. Fenzi, C. Bourdelle, G. Falchetto, X. Garbet, T. Aniel, F. Clairet, R. Sabot, Nuclear Fusion 48 (2008).
[40] V. Bulanin, A. Petrov, M. 'Yefanov, in: 30th EPS Conf. Plasma Phys., vol. 27J, 2003.
[41] F. da Silva, S. Heuraux, N. Lemoine, C. Honoré, P. Hennequin, M. Manso, R. Sabot, Rev. Sci. Inst. 75 (2004) 3816.
[42] E. Blanco, T. Estrada, Plasma Physics and Controlled Fusion 50 (2008) 095011.
[43] C. Lechte, IEEE Trans. Plasma Sci. 37 (2009) 1099.